RAPID COMMUNICATIONS

PHYSICAL REVIEW B VOLUME 50, NUMBER 22 1 DECEMBER 1994-II

Static and dynamic mechanisms of the anomalous field dependence of magnetization in Bi-Sr-Ca-Cu-O and Bi-Pb-Sr-Ca-Cu-O single crystals

X. Y. Cai, A. Gurevich, D. C. Larbalestier, R. J. Kelley, and M. Onellion
Applied Superconductivity Center, University of Wisconsin, Madison, Wisconsin 53706

H. Berger and G. Margaritondo
Institut de Physique Appliquee, Ecole Polytechnique Federale, CH-1015 Lausanne, Switzerland
(Received 12 September 1994)

We have measured and analyzed both the static and dynamic contribution to the anomalous nonmonotonic dependence of the irreversible magnetization, $M(B)$, for underdoped $Bi_2Sr_2CaCu_2O_{8+y}$ and overdoped $(Bi_{1.6}Pb_{0.4})Sr_2CaCu_2O_{8+y}$ single crystals. We extracted the "unrelaxed" magnetization $M_c(B)$ and traced the time evolution of $M(B,t)$ from short to long time scales using combined magnetization and flux-creep measurements. Despite their large differences in anisotropy, pinning force, and flux-creep rate $s(B)=d\ln M/d\ln t$, both samples showed the anomaly over a wide range of T, the anomaly being most pronounced in the "unrelaxed" state. This suggests that the primary cause of the anomaly lies in the flux-pinning defect structure of the material. However, $M(B,E)$ also essentially depends on the induced electric field E in the sample, so the shape of the $M(B)$ curve can strongly change with time due to the relaxation of $E(t)$ and the nonmonotonic dependence of $s(B)$.

The nonmonotonic field dependence of the magnetization $M(B)$ (the so-called "fishtail" or "peak-effect" anomaly) in high-T_c superconductors (HTS) has attracted much attention.[1–10] Several explanations have been proposed within the framework of both static[1–6] and dynamic[7–9] mechanisms. Static interpretations tend to emphasize flux pinning, ascribing the observed anomaly to the increase of the bulk pinning force with B in a certain field region. This could be due to inhomogeneities of T_c, so that the regions with reduced T_c become normal as B is increased.[1,3] Other reasons for the anomaly might be the surface barrier,[2,7] or the decomposition of line vortices into two-dimensional (2D) pancake vortices above a decoupling field B_d.[4] In the dynamic scenario, the experimentally observed $M(B)$ is determined by fast flux creep from the "unrelaxed" $M_c(B)$ which is assumed to decrease monotonically with B. In this case the anomaly is due to the nonmonotonic dependence of the flux-creep rate $s(B)=d\ln M/d\ln t$ on B.[8,9] Distinguishing unambiguously between these possibilities is complex because all these mechanisms seem to contribute to the anomalous behavior of $M(B)$ in HTS. For instance, the short coherence length makes HTS sensitive to virtually any crystalline disorder, especially to oxygen defects which strongly affect T_c.[1,3] In addition, the large anisotropy of HTS can give rise to a dimensional crossover between 2D and 3D pinning regimes, and the strong flux creep makes $M(B)$ dependent both on the shape of the current-voltage (I-V) characteristic and on the electric field, E, in the sample.

The fact that $s(T,B)\ll 1$ below the irreversibility line implies that the critical state model remains approximately valid; however, $s(T,B)$ in HTS is not small enough to neglect the essential dependence of M on E. This brings about features which this model does not take into account; in particular, the critical current densities $J_c(B)$ observed in resistive and magnetization measurements can be quite different, as they correspond to different electric field criteria E_c and E_m. Here E_c is usually taken as 1 μV/cm, while $E_m\sim\dot{B}_e a$ is proportional to the magnetic ramp rate $\dot{B}_e$ and a sample size, a, with E_m usually being smaller than E_c by several orders of magnitude. If M is measured at the fixed B, the internal electric field $E_r(t,B)\simeq(t_0/t)^{1+s}E_c$ is not only much smaller than E_m, but it also decays with time t due to flux creep and becomes dependent on B and T. Here $t_0(B,T)$ is a macroscopic time constant, and E_r was taken for the power-law I-V curve, $E=E_c(J/J_c)^n$, for which $s=1/(n-1)$ (Ref. 11) (see below). Therefore, $M(B,E_r(B,t))$ obtained from flux-creep measurements can also differ from $M(B,E_m)$ and $M(B,E_c)$, that is, the apparent field dependence of $M(B)$ can be strongly affected by the internal electric field. Due to the time decay of $E(t)$ in the flux-creep regime, different E correspond here to different time scales $t(E)\simeq t_0(E_c/E)^{1/(1+s)}$, so that $M(B,E)$ can be obtained from the observed relaxation curves $M(B,t)$ by replacing t by $t(E)$.[11]

In this paper we reconstruct $M(B)$ for different E from combined resistive, magnetization and flux-creep measurements. This allows us to separate the static and dynamic contributions to $M(B)$; in particular, to extract the "unrelaxed" $M_c(B)$ and to trace the evolution of $M(B,E)$ upon changing $\dot{B}_e$ and the experimental time window. To study the effect of doping, flux pinning and anisotropy, we compare a highly anisotropic, underdoped $Bi_2Sr_2CaCu_2O_{8+y}$ (BSCCO) and a much less anisotropic, overdoped $(Bi_{1.6}Pb_{0.4})Sr_2CaCu_2O_{8+y}$ (BPSCCO) single crystals.

The samples were prepared by a standard flux-grown technique; the underdoped, vacuum-annealed BSCCO crystal had a size of $1\times0.93\times0.015$ mm^3, the onset $T_c=86$ K, the width of the resistive transition $\Delta T_c(B=0)\approx2$ K, and the ratio of the out-of-plane to the in-plane resistivities, $\rho_c/\rho_{ab}\approx10^5$ at $T=T_c$. The BPSCCO crystal had dimensions $1.6\times1.6\times0.04$ mm^3, $T_c=74$ K, $\Delta T_c\approx5$ K, and $\rho_c/\rho_{ab}\approx10^3$.

Measurements of $M(B)$ were performed with **H** directed parallel to the c axis in a Quantum Design superconducting

0163-1829/94/50(22)/16774(4)/$06.00

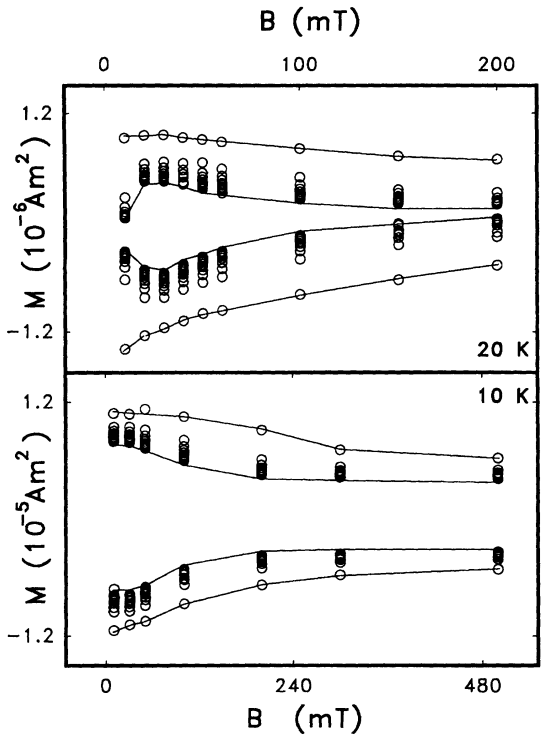

FIG. 1. Magnetization curves for the $Bi_2Sr_2CaCu_2O_{8+y}$ crystal measured at 10 and 20 K at times varying from 60 to 6000 s in both increasing and decreasing fields. The outer curves correspond to the initial measurements. Note the different field scales at different T.

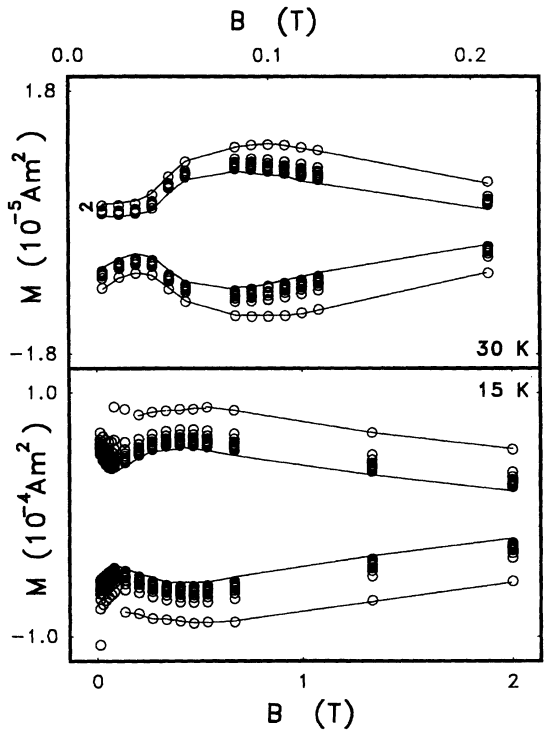

FIG. 2. Magnetization curves for the $(Bi_{1.6}Pb_{0.4})Sr_2CaCu_2O_{8+y}$ crystal measured at 15 and 30 K at times varying from 60 to 6000 s in both increasing and decreasing fields. The outer curves correspond to the initial measurements. Note the different field scales at different T and their larger magnitude as compared to the similar curves in Fig. 1.

quantum interference device (SQUID) magnetometer according to two different protocols, so as to verify that the relaxation of $M(B_n,t)$ was independent of the previous magnetization state, $M(B_{n-1},t)$. In both cases, the crystals were zero field cooled, and then the magnetic field was increased to the nth data point B_n at a ramp rate $\dot{B}_e=0.01$ T/min. Then $B(t)$ was fixed and the relaxation of $M(t)$ was measured within the time window $t_i<t<t_f$, where $t_i\approx 60$ s, and $t_f=6000$ s. After that, B was incremented to the next field B_{n+1}, first in increasing and then in decreasing fields, and the procedure repeated. In the second scheme, we decreased B to zero after making each set of flux-creep measurements, warmed the sample above T_c, recooled the sample and then ramped the field with the same rate $\dot{B}_e$ to the next point $B=B_{n+1}$. The results were identical for both methods. We excluded the region of incomplete flux penetration, $B<B_p(T)\approx\mu_0 J_c d$, where d is the sample thickness, and $B_p(T)$ varies from 50 to 500 Oe.

Figures 1 and 2 show representative examples of $M(B,t)$ curves. For underdoped BSCCO, the anomaly in $M(B,t)$ was almost absent at the shortest measured times, but it gradually developed with time. Similar behavior was reported by Yeshurun *et al.*[9] However for overdoped BPSCCO, the short-time anomaly was much more pronounced, especially at 30 K, where a strong peak effect in $M(B)$ was observed within the entire time window. The relaxation of $M(t)$ was well described in all cases by the power-law $M\propto t^{-s(T,B)}$, as also observed for Bi-based HTS.[12,13] This fact is important for further analysis, since it enables us to reconstruct $M(B,t)$ well outside the experimental time window by extrapolating the steady-state relaxation curves

$$\ln M(T,B,t)=\ln M_c(T,B)-s(T,B)\ln(t/t_0) \qquad (1)$$

to different time scales, as shown in Figs. 3(a) and 4(a). The creep rate, $s(T,B)=d\ln M/d\ln t$ is equal to the tangent of the lines in Figs. 3(a) and 4(a) and is shown in the insets.

To clarify the meaning of M_c and t_0 in Eq. (1), we consider two characteristic flux-creep time scales t_0 and τ determined by nonlinear flux diffusion.[11] For the power-law V-I characteristic, $E\propto J^n$, the values of t_0 and τ are given by

$$t_0=\frac{\alpha\mu_0 M_c s}{AE_c}, \quad \tau=\beta t_0\left(\frac{E_c}{a\dot{B}_e}\right)^{1/(s+1)}, \qquad (2)$$

where M_c corresponds to the electric field E_c, and A and a are the area and the size of the sample side perpendicular to the magnetic field, respectively, and the numerical coefficients $\alpha\sim 1$ and $\beta\sim 1$ depend on the sample geometry. Here τ determines the initial transient stage of flux creep needed for a diffusive redistribution of magnetic flux over the sample cross section at the given induced field $E(0)\sim a\dot{B}_e$, while the extrapolation of the steady state $\ln M(\ln t)$ back to $t=\tau$ yields the initial magnetic moment $M(0,B_e)$.[11] Next, we define an electric field E_c, above which the power approximation of the I-V curve is no longer valid, because there is a crossover between the flux-creep and flux-flow regimes. This critical field E_c determines the time constant t_0 which corresponds to the maximum ramp

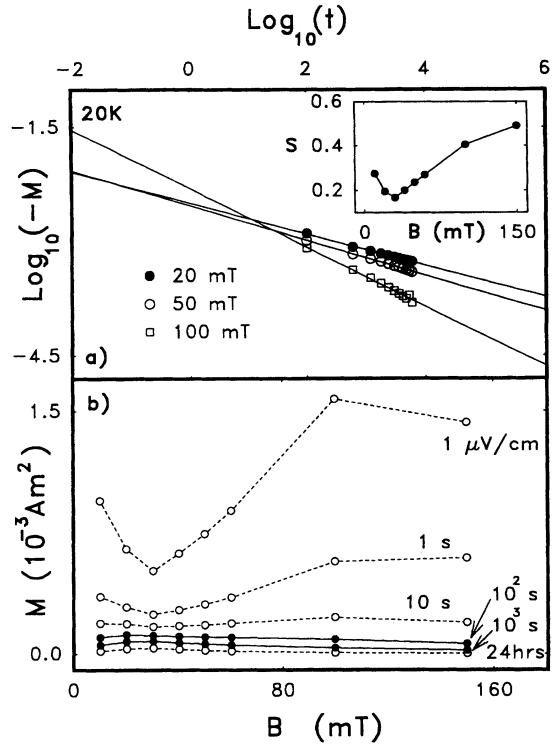

FIG. 3. Examples of the power-law relaxation of $M(t)$ in $Bi_2Sr_2CaCu_2O_{8+y}$ and the linear extrapolation of $\ln M(\ln t)$ beyond the experimental time window (a). Measured points are shown together with the extrapolated lines outside the experimental time window. The curve labeled by 1 μV/cm corresponds to $M_c(B)$ as calculated from Eq. (3).

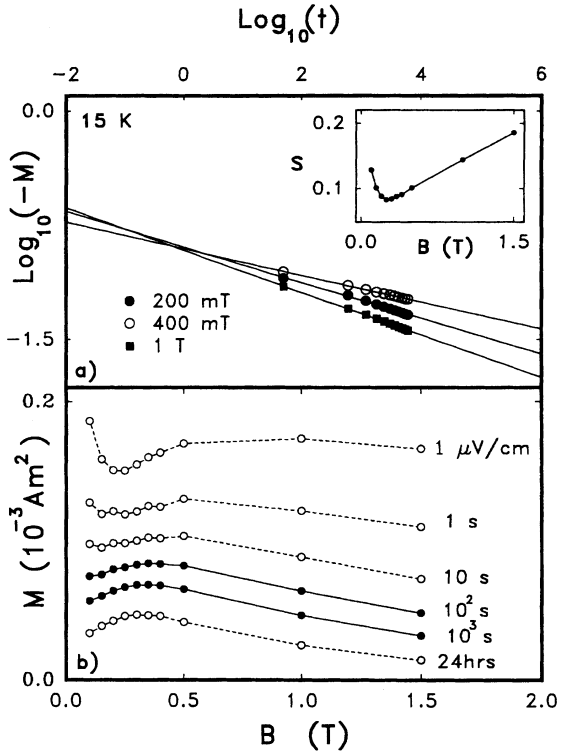

FIG. 4. Examples of the power-law relaxation of $M(t)$ in $(Bi_{1.6}Pb_{0.4})Sr_2CaCu_2O_{8+}$ and the linear extrapolation of $\ln M(\ln t)$ beyond the experimental time window (a). Measured points are shown together with the extrapolated lines outside the experimental time window. The curve labeled by 1 μV/cm corresponds to $M_c(B)$ as calculated from Eq. (3).

rate $\dot{B}_e \sim E_c/a$ for which the superconductor still remains in the flux-creep regime. The extrapolation of $\ln M(\ln t)$ back to $t=t_0$ gives the quantity $M_c=M(B,E_c)$, which is independent of $\dot{B}_e$ and which corresponds to the electric field E_c above which the whole vortex structure gets depinned. Therefore, M_c can be regarded as the "unrelaxed" magnetic moment which is principally determined by static flux pinning. For BSCCO, the power-law $E(J)$ was observed in a wide region of E, from 10^{-5}–10^{-6} to 0.1 μV/cm,[13] thus showing that the crossover occurs at higher E. At the same time, our transport measurements of $E(J)$ on the BSCCO crystal shown in Fig. 5 indicate the beginning of flux flow above $E \sim 20$–50 μV/cm. Thus, the crossover region occupies about 2–3 decades in E, so for further qualitative analysis we assume the conventional criterion $E_c=1$ μV/cm for J_c, recognizing that the results are not very sensitive to the particular value of E_c and the details of the crossover region, as shown below.

For $\dot{B}_e=0.01$ T/min, $a=1$ mm, $A=1$ mm^2, $s=0.1$, and $E_c=1$ μV/cm, we find that 0.1 ms$<t_0<$0.1 s and 0.1 $<\tau<$100 s if M_c ranges from 10^{-4} to 0.1 emu (see Figs. 1 and 2). Since t_0 is much smaller than τ, the lines $\ln M(\ln t)$ should be extrapolated back to $t=t_0$ from $t_i \approx 60$ s by 2–3 decades to obtain $M_c(B)$. Substituting $t=t_i$ in Eq. (1) and using Eq. (2) for t_0, we obtain M_c in the form

$$M_c=\left(\frac{At_iE_cM_i^{1/s}}{\mu_0\alpha s}\right)^{s/(1+s)}. \tag{3}$$

For $s(B)\ll 1$, a superconductor is almost in the critical state, so M_c is not very sensitive to the exact values of α and E_c (for instance, at $s=0.1$, the change of E_c/α by 10 times causes the change of M_c by 23%), and instead of M_i and t_i one can take any other data point (M_n,t_n).

The linear dependence of $\ln M$ on $\ln t$ in Figs. 3(a) and 4(a) permits us to extrapolate $M(\ln t)$ to long times as well, and thereby to obtain $M(B)$ even beyond the "human" time window. Although the applicability limits of the power-law I-V curve, $E \propto J^n$, at small J are generally unknown, the good fit within the experimental time window in Figs. 3(a) and 4(a) suggests that it is reasonable to assume the power-law relaxation $M \propto t^{-s}$ to remain valid at least within the next 1–2 decades. There are both theoretical[14,15] and experimental[12,13] evidences for the power-law $E(J)$ for highly anisotropic Bi-based HTS, although, at small J, plastic effects due to edge dislocations in the vortex structure can markedly affect $E(J)$.[15] Therefore, the linear extrapolation of $\ln M(\ln t)$ gives $M(B,t)$ for all flux-creep time scales $t_c<t<t_{\max}$, where $t_{\max} \sim \mu_0 a^2 J_c s/E_{\min}$ corresponds to the electric field, $E_{\min}$, below which the plastic effects modify the power dependence $E(J)$. Thus this scheme enables reconstruction of a significant portion of the whole $M(B,t)$ surface from the small portion accessible in the experimental time window.

Figures 3(b) and 4(b) show the time evolution of $M(B)$ from below to beyond the experimental time window. De-

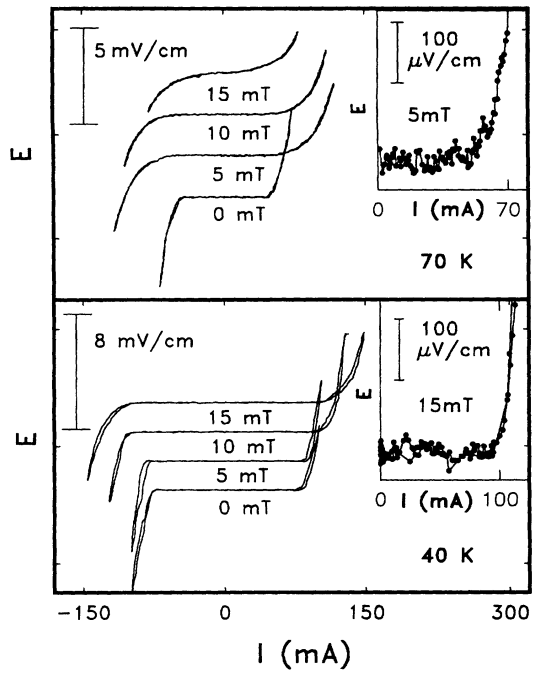

FIG. 5. V-I curves of $Bi_2Sr_2CaCu_2O_{8+y}$ at 40 and 70 K which clearly show the increase of J_c with B. Insets show characteristic thresholds of the flux-flow regimes.

spite the large difference in anisotropy, pinning force, and creep rate for the two crystals, they exhibit remarkably similar qualitative behavior. In both cases, the "fishtail" anomaly is most pronounced in the "unrelaxed" $M_c(B)$ determined by static flux pinning. Subsequent relaxation smoothes out the nonmonotonic dependence $M(B)$ until it almost disappears at a certain time ($t=t_c\sim 10$ s for both samples), after which, the anomaly appears again due to the minimum in $s(B)$. Such a dependence of s on B was attributed by Krusin-Elbaum *et al.*[8] to a crossover from single-vortex to collective flux-creep regimes. The fields $B_{\min}$ and $B_{\max}$ at which $M(B)$ passes through minimum and maximum, respectively, decrease with time. For underdoped BSCCO, both $B_{\min}$ and $B_{\max}$ weakly depend on T, but for overdoped BPSCCO those dependencies are much stronger.

For $t>t_i$, the curves $M(B,t)$ shown in Figs. 3(b) and 4(b) are similar to those which have previously been observed for HTS,[8,9] though our interpretation differs from that of Refs. 8 and 9. Indeed, the fact that the "fishtail" anomaly becomes least pronounced for shorter times, was interpreted in Ref. 9 as evidence of its absence at $t\ll t_i$, the anomaly thus being a consequence of flux creep at $0<t<t_i$. In this case the initially measured value $M(B,t_i)$ was regarded as M_c, but, as shown here, $M_c(B)$ can significantly differ from the value $M(B,t_i)$ which depends on t_i and $\dot{B}_e$. Meanwhile, the above extrapolation of the *steady-state* ($t\gg\tau$) curves $\ln M(\ln t)$ to different time scales enables us to extract $M_c(B,T)$ and to show that the fishtail anomaly in $M(B)$ for both over- and underdoped crystals is present at any t (or E). This was also confirmed by direct transport measurements of the I-V curves of the BSCCO crystal. Figure 5 shows that these have a nonmonotonic dependence $J_c(B)$ at $E>50$ μV/cm at 40 and 70 K. The anomaly in both transport and magnetization data has also been reported by Gordeev *et al.*[10] for $YBa_2Cu_3O_7$. Thus, the evolution of $M(B,t)$ results from a complex interplay of static and dynamic effects, where flux pinning determines the initial nonmonotonic dependence of M_c on B, while the subsequent flux creep can strongly affect the shape of $M(B)$ due to the large values of $s(B)$. We believe that the static anomaly in $M_c(B)$ can be due to regions of varying O content, similar to those in $YBa_2Cu_3O_7$ (Refs. 1 and 16) and $La_{2-x}Sr_xCuO_{4+y}$.[17] At the same time, the qualitatively analogous behavior of $M(B,t)$ for underdoped BSCCO and overdoped BPSCCO having very different anisotropy seems to indicate that the anisotropy is a contributory, rather than the primary mechanism of the "fishtail" anomaly.

We are grateful to L. Krusin-Elbaum, E. Kadyrov, and J. L. Vargas for discussions. The work at the University of Wisconsin was supported by the NSF Materials Research Group Program (DMR-9214707) and that at the EPFL by Fonds National Suisse de la Recherche Scientifique.

[1] M. Daeumling, J. M. Seuntjens, and D. C. Larbalestier, Nature (London) **346**, 332 (1990); J. L. Vargas and D. C. Larbalestier, Appl. Phys. Lett. **60**, 1741 (1992).

[2] V. N. Kopylov, A. E. Koshelev, I. F. Schegolev, and T. G. Togonidze, Physica C **170**, 291 (1990).

[3] M. S. Osofsky *et al.*, Phys. Rev. B **45**, 4916 (1992); J. G. Ossandon *et al.*, *ibid.* **45**, 12 534 (1992); L. Klein *et al.*, *ibid.* **49**, 4403 (1994).

[4] T. Tamegai, Y. Iye, I. Oguro, and K. Kishio, Physica C **213**, 33 (1993).

[5] G. Yang *et al.*, Phys. Rev. B **48**, 4054 (1993).

[6] L. F. Cohen *et al.*, Cryogenics **33**, 352 (1993); A. D. Caplin, L. F. Cohen, G. K. Perkins, and A. A. Zhukov, Supercond. Sci. Technol. **7**, 412 (1994).

[7] N. Chikumoto, M. Konczykowski, N. Motohira, and A. P. Malozemoff, Phys. Rev. Lett. **69**, 1260 (1992).

[8] L. Krusin-Elbaum, L. Civale, V. M. Vinokur, and F. Holtzberg, Phys. Rev. Lett. **69**, 2280 (1992).

[9] Y. Yeshurun, N. Bontemps, L. Burlachkov, and A. Kapitulnik, Phys. Rev. B **49**, 1548 (1994).

[10] S. N. Gordeev *et al.*, Phys. Rev. B **49**, 15 420 (1994).

[11] A. Gurevich *et al.*, Phys. Rev. B **44**, 12 090 (1991); A. Gurevich and H. Kupfer, *ibid.* **48**, 6477 (1993); A. Gurevich and E. H. Brandt, Phys. Rev. Lett. **73**, 178 (1994).

[12] C. J. van der Beek *et al.*, Physica C **195**, 307 (1992).

[13] A. A. Zhukov *et al.*, Physica C **219**, 99 (1994).

[14] D. S. Fisher, M. P. A. Fisher, and D. A. Huse, Phys. Rev. B **43**, 130 (1991).

[15] M. V. Feigelman, V. B. Geshkenbein, and A. I. Larkin, Physica C **167**, 117 (1990); V. M. Vinokur, P. H. Kes, and A. E. Koshelev, *ibid.* **168**, 29 (1990).

[16] S. Semenovskaya and A. G. Khachaturyan, Phys. Rev. B **46**, 6511 (1992).

[17] T. Kobayashi *et al.*, Appl. Phys. Lett. **62**, 1830 (1993).